

## LARGE EDDY SIMULATION OF PREMIXED AND NON-PREMIXED COMBUSTION

**W. Malalasekera**

Wolfson School of Mechanical and Manufacturing  
Engineering, Loughborough University  
Loughborough, Leics, LE11 3TU, UK.  
w.malalasekera@lboro.ac.uk

**S.S. Ibrahim**

Department of Aeronautics and Automotive  
Engineering, Loughborough University,  
Loughborough Leics, LE11 3TU, UK  
s.s.ibrahim@lboro.ac.uk

**A.R. Masri**

School of Aerospace Mechanical and Mechatronic  
Engineering  
University of Sydney  
Sydney, NSW 2006, Australia.

**S. K. Sadasivuni<sup>1</sup>**

Wolfson School of Mechanical and Manufacturing  
Engineering, Loughborough University  
Loughborough, Leics, LE11 3TU, UK.

**S. R. Gubba**

CFD centre, School of Process, Environment and  
Materials Engineering, University of Leeds, Leeds, LS2 9JT, UK  
S.R.Gubba@leeds.ac.uk

<sup>1</sup> Present address: Siemens Industrial Turbo Machinery (SIT) Ltd, Ruston House, Waterside South, Lincoln LN5 7FD, England

### ABSTRACT

This paper summarises the authors experience in using the Large Eddy Simulation (LES) technique for the modelling of premixed and non-premixed combustion. The paper describes the application of LES based combustion modelling technique to two well defined experimental configurations where high quality data is available for validation. The large eddy simulation technique for the modelling flow and turbulence is based on the solution of governing equations for continuity and momentum in a structured Cartesian grid arrangement. Smagorinsky eddy viscosity model with a localised dynamic procedure is used as the sub-grid scale turbulence model. A swirl flame is considered as the non-premixed combustion application. For non-premixed combustion modelling a conserved scalar

mixture fraction based steady laminar flamelet model is used. A radiation model incorporating the discrete transfer method is included in the non-premixed swirl flame calculations. For premixed combustion where the application considered here is flame propagation in a confined explosion chamber, a model based on dynamic flame surface density (DSFD) is used. It is shown that in both cases LES based combustion models perform remarkably well and results agree well with the experimental data.

Keywords: Large eddy simulation (LES), Swirl, Combustion Modelling, Premixed, Non-premixed

### INTRODUCTION

Advancement in the design and operation of combustion devices used in automobile, air

transport and power generation industries is very important for the reduction of emissions contributing to global warming. Such advances depend upon making combustion equipment operate at higher efficiencies so that more power can be extracted for the same amount of fuel burnt. This will, in the long run, reduce emissions or maintain at the present levels while meeting the present and future demand for power and energy. To this end Computational Fluid Dynamics (CFD) has become a vital tool in the design process and more and more industries are now using CFD to explore flow behaviour of various designs and simulate temperature, heat transfer and emissions in combustion equipment before prototypes are built for testing. Such CFD studies have various benefits – design cycle can be shortened, new ideas can be tested without prior experimentation which can be very costly and incremental changes can be made to the design to achieve a desired effect.

There are many issues that make combustion modelling one of the most difficult areas in CFD applications. Complexities such as turbulence/chemistry interactions, chemical kinetics, coupling of flow turbulence and temperature to density, heat transfer and radiation effects make the CFD modelling of combustion very challenging. The interaction of turbulence and chemistry plays an important role in premixed as well as non-premixed combustion situations. Therefore success in combustion modelling in many situations depends on the success in turbulence modelling. Until recently RANS based flow models coupled with various types of combustion models to suit the application area have been used with some success in industrial applications. However in more complex situations such as strong swirling flows and highly dynamics propagating flames, success of the RANS based models has been limited. This paper summarises application of LES based combustion modelling techniques to cases where RANS based modelling has resulted in limited success due to complexity of the flow configuration. For premixed combustion simulations a propagating flame in a confined explosion chamber with obstacles is considered. For non-premixed, the application of LES for the modelling of a swirl stabled flame is considered.

For both cases experimental data sets for validation have been obtained from the experiments conducted at the Sydney University.

## **Modelling of Swirl Flames**

Swirl stabilised turbulent flames are widely used in a range of practical combustion applications such as gas turbines, furnaces, power station combustors and boilers. The complexity of the resulting flames in swirl flame situations depend on the strength of swirl and the method of swirl generation. In many cases a number of recirculation zones and a central vortex break-down (VB) region can be seen in swirl stabilised flames. Recirculation zones in swirl stabilised flames are effective in providing a source of well mixed combustion products and act as storage of heat and chemically active species to sustain combustion and provide flame stabilization. Another type of a coherent structure referred to as precessing vortex core (PVC) which is an asymmetric three-dimensional time dependent flow structure is also present in some high swirl number flows. In general these features make swirl flows and flames to exhibits highly three-dimensional, large scale turbulent structures with complex turbulent shear flow regions. Modelling of and accurate prediction of such complex details remains a challenge and LES based CFD and combustion modelling techniques have various advantages over RANS based models. Many experimental and theoretical studies have been conducted to understand features of swirl flows (Syred and Beer, 1974, Gupta et al., 1984, Escudier, 1988, Lucca-Negro and O'Doherty, 2001). Numerical calculation of swirl flows has also received considerable attention. Majority of the attempts have used Reynolds averaged Navier-Stokes (RANS) equations accompanying different turbulence models to predict swirl flows. Reviews by Sloan et al. (1986) and Weber et al. (1990) have summarised these attempts. In general RANS based models are primarily suitable to calculate stationary flows with non-gradient transport and they are not capable of capturing the unsteady nature of the large-scale flow structures found in swirl flows. Large eddy simulation (LES) technique solves for large scale unsteady behaviour of

turbulent flows therefore it is a promising numerical tool to accurately predict complex turbulent flows. Among others, the studies of Kim et al. (1999), Sankaran and Menon (2002), Di Mare et al. (2004), Wall and Moin (2005), Mahesh et al. (2005) have demonstrated the ability of LES to capture detailed flow field in swirling flow configurations.

### Modelling of Propagating Premixed Flames

Premixed combustion is encountered in many engineering applications such as spark ignition engines, gas turbines and accidental explosion events. Outstanding research issues associated with understanding the structure of the flame front and the combustion regimes as the flame front propagates through highly turbulent flow field are further complicated by instabilities, which occur due to the unsteady nature of the flow. Understanding such issues is central to the development of advanced physical sub-models that improve current predictive capabilities for turbulent premixed flames. Here we consider a laboratory scale experimental vented explosion situation and apply the large eddy simulation technique to predict experimentally obtained data. Previous applications of RANS based models to the same geometrical configuration have shown the limitations of RANS based models (Patel et al, 2004). LES based models are now accepted as feasible computational tools in modelling propagating premixed turbulent combustion problems (Masri et al, 2006, Charlette, et al, 2002, Fureby et al., 2005, Knikker et al, 2002, and Pitsch, 2005). LES has a clear advantage over classical Reynolds averaged methods in the capability of accounting for time-varying nature of flows and this is particularly important in transient processes such as turbulent premixed propagating flames. Ever increasing speed of processors and the availability of parallel computing hardware make the LES technique a very useful tool for accurate modelling of highly turbulent combusting flows, such as propagating premixed flames

## MATHEMATICAL MODELS

### Equations solved

Large eddy simulations demonstrate accurate and more sophisticated methodology for turbulence

calculations compared to Reynolds Averaged Navier Stokes (RANS) based modelling. LES resolves the large scale turbulent motions which contain the majority of turbulent kinetic energy and control the dynamics of turbulence, whereas the small scales or sub-grid scales are modelled. The advantage of resolving the large scale motion is not applicable to chemical source term as the chemical time scales are smaller and therefore combustion needs to be modelled. However, LES seems to have the advantages over RANS due to its ability to predict accurately the intense scalar mixing process in most complex flows.

In LES the governing equations which resolve the large scale features are obtain by applying a filtering operator. A number of filters are used in LES and a top hat filter having the filter-width  $\bar{\Delta}_j$  set equal to the size  $\Delta x_j$  of the local cell is used in the present work. The transport equations for Favre filtered mass, momentum are given by:

$$\frac{\partial \bar{\rho}}{\partial t} + \frac{\partial \bar{\rho} \tilde{u}_j}{\partial x_j} = 0 \quad (1)$$

$$\frac{\partial \bar{\rho} \tilde{u}_i}{\partial t} + \frac{\partial (\bar{\rho} \tilde{u}_i \tilde{u}_j)}{\partial x_j} = -\frac{\partial \bar{P}}{\partial x_i} + \frac{\partial}{\partial x_j} \left[ \bar{\rho} \nu \left( \frac{\partial \tilde{u}_i}{\partial x_j} + \frac{\partial \tilde{u}_j}{\partial x_i} \right) - \frac{2}{3} \bar{\rho} \frac{\partial \tilde{u}_k}{\partial x_k} \right] + \frac{\partial \tau_{ij}}{\partial x_j} \quad (2)$$

### Turbulence Model

The sub-grid contribution to the momentum flux is computed using Smagorinsky eddy viscosity model (Smagorinsky, 1963) which uses a model constant  $C_s$ , the filter width  $\bar{\Delta}$  and strain rate tensor  $S_{i,j}$  according to equation (3):

$$\nu_t = C_s \bar{\Delta}^2 |S_{i,j}| = C_s \bar{\Delta}^2 \left| \frac{1}{2} \left( \frac{\partial \tilde{u}_i}{\partial x_j} + \frac{\partial \tilde{u}_j}{\partial x_i} \right) \right| \quad (3)$$

In the present work the model parameter  $C_s$  is obtained through a localised dynamic procedure depending on the application. (Piomelli and Liu, 1995, Moin et al, 1991).

### Combustion Model: Non-premixed

In combustion, the chemical reactions occur mostly in the sub-grid scales and therefore consequent

modelling is required for combustion chemistry. In this work the Steady Laminar Flamelet Model (SLFM) is used to form the combustion modelling aspect. Here a presumed probability density function (PDF) of the mixture fraction is chosen as a means of modelling the sub-grid scale mixing. The transport equation for conserved scalar mixture fraction is written as

$$\frac{\partial \tilde{\rho} \tilde{f}}{\partial t} + \frac{\partial}{\partial x_j} (\tilde{\rho} \tilde{u}_j \tilde{f}) = \frac{\partial}{\partial x_j} \left[ \tilde{\rho} \left( \frac{\nu}{\sigma} + \frac{\sigma_t}{\sigma} \right) \frac{\partial \tilde{f}}{\partial x_j} \right] \quad (4)$$

In the above equations  $\rho$  is the density,  $\tilde{u}_i$  is the velocity component in  $x_i$  direction,  $p$  is the pressure,  $\nu$  is the kinematics viscosity,  $f$  is the mixture fraction,  $\nu_t$  is the turbulent viscosity,  $\sigma$  is the laminar Schmidt number,  $\sigma_t$  is the turbulent Schmidt number. A  $\beta$  function is used for the mixture fraction PDF. The functional dependence of the thermo-chemical variables is closed through the steady laminar flamelet approach. In this approach the variables, density, temperature and species concentrations only depend on Favre filtered mixture fraction, mixture fraction variance and scalar dissipation rate. The sub-grid scale variance of the mixture fraction is modelled assuming the gradient transport model proposed by Branley and Jones (2001) The flamelet calculations have been performed using the Flamemaster code (Pitsch, 1998) incorporating the GRI 2.11 mechanism for detailed chemistry (Bowman et al, 2006). Further details can be found in Malalasekera et al. (2009).

Many combustion simulations tend to ignore the effect of radiation in the calculations. This is because the governing radiative transfer equation is of integro-differential nature makes the analysis difficult and computationally expensive. The well known Discrete Transfer Method (DTM), Lockwood and Shah (1981) and Shah (1979), is used as the radiation calculation algorithms in this work. This is a ray-based calculation method and in our previous work we have established the accuracy and advantages of this method when applied to large and complex problems (Malalasekera, and James, 1996, Malalasekera and Henson, 1997, Henson, 1998). The absorption coefficient is calculated from LES data using

transient temperature and relevant species distributions. For this the Mixed Grey Gas Model of Truelove (1976), is used in the present study. The major computational effort in the discrete transfer method is to trace rays through cell volumes in the discretised radiation space. An efficient and fast ray calculation algorithm used in our previous studies (Malalasekera, and James, 1996, Malalasekera and Henson, 1997) is employed in this work. Although transient calculation of radiation is computationally very expensive the algorithm we use is devised in such a way that ray data are calculated only once and stored to re-use in each radiation calculation at every time step with updated temperature and absorption coefficient data.

### Combustion model: Premixed

As mentioned above, in LES, large eddies above a cut-off length scale are resolved and the small ones are modelled by assuming isotropic in nature, using sub-grid scale (SGS) models. For premixed combustion simulations presented here Favre filtered (density weighted) conservation equations of mass, momentum, energy and a transport equation for the reaction progress variable are solved together with the state equation. Turbulence is modelled using the classical Smagorinsky model (Smagorinsky, 1963) and the model coefficient is calculated from instantaneous flow conditions using the dynamic determination procedure developed by Moin et al. (1991), for compressible flows.

In the application considered here modelling of the mean chemical reaction rate in deflagrating flames is very challenging due to its non-linear relation with chemical and thermodynamic states, and often characterised by propagating thin reaction layers thinner than the smallest turbulent scales. The major difficulty in the modelling of reaction rate is due to sharp variation of thermo chemical variables through the laminar flame profile, which is typically very thin (Veynante and Poinot, 1997). This issue is strongly affected by turbulence, which causes flame wrinkling and thereby forming the most complex three way thermo-chemical-turbulence interactions. However, assuming single step irreversible chemistry and the Zeldovich

instability (thermal diffusion), i.e. unity Lewis number will reduce the complexity of the whole system. The chemical state is then described by defining the reaction progress variable  $\tilde{c}$  from zero to one in unburned mixture and products respectively, based on fuel mass fraction. Mathematically it can be derived as,  $1 - Y_{fu} / Y_{fu}^0$ . Here  $Y_{fu}$  is the local fuel mass fraction and  $Y_{fu}^0$  is the fuel mass fraction in unburned mixture. The mean SGS chemical reaction rate  $\overline{\dot{\omega}_c}$  in the reaction progress variable equation (not shown here) is modelled by following the laminar flamelet approach as:

$$\overline{\dot{\omega}_c} = \rho_u u_L \overline{\Sigma} \quad (5)$$

where  $\rho_u$  is the density of the unburned mixture,  $u_L$  is the laminar burning velocity, and  $\overline{\Sigma}$  is the flame surface density. Flame surface density models have been used in the RANS context to predict similar premixed combustion problems (Patel et al, 2004). Here this approach is extended to LES. In this work the LES combustion model is based on dynamic determination of the resolved and unresolved flame surface density (FSD), which allows for the sub-grid scale (SGS) dynamic effects of the local flame interactions. Following the authors recent work (Gubba et al, 2008, Ibrahim et al, 2009) a novel dynamic flame surface density (DFSD) model (Knikker et al, 2004), is used for premixed combustion modelling work described here to calculate the reaction rate given by equation (5). Further details are available in Ibrahim et al. (2009).

## EXPERIMENTAL AND COMPUTATIONAL DETAILS

### Sydney Swirl Burner

Sydney swirl flame experiments provide a high quality experimental database for the validation of computations (Al-Abdeli and Masri, 2003, Masri et al, 2004). Figure 1 (a) shows the experimental configuration of the Sydney swirl burner. The burner has a 3.6mm diameter central jet with a 50mm diameter bluff body surrounding it. Swirl flow generated downstream by means of inclined radial jets enters the burner level through an

annulus around the bluff body as shown in the figure. The swirl annulus covers the bluff body with an outer diameter of 60mm. The entire burner is placed in a tunnel with an air flow with low velocity. This enables the modellers to set very well defined boundary conditions in their computations. The dimensions of the tunnel are 250 x 250 (mm). From this experimental series flames known as SMH1 and SMH2 are the two flames widely used for validation of combustion simulations in swirl flames. These two flames have the same burner configuration, but different flow conditions. Detail description of the burner parameters and its operation is available in the above references. The SMH1 flame with flame operating conditions shown in Table 1 is considered for the present calculations. In this flame the fuel jet consists of CH<sub>4</sub>/H<sub>2</sub> with an inlet jet velocity ( $U_j$ ) of 140.8 m/s. A swirl number of 0.32 is maintained for the swirl inlet with an axial velocity ( $U_s$ ) and tangential velocity ( $W_s$ ) components of 42.8 m/s and 13.8 m/s respectively. The external ambient co-flow velocity of 20 m/s ( $U_c$ ) is provided.

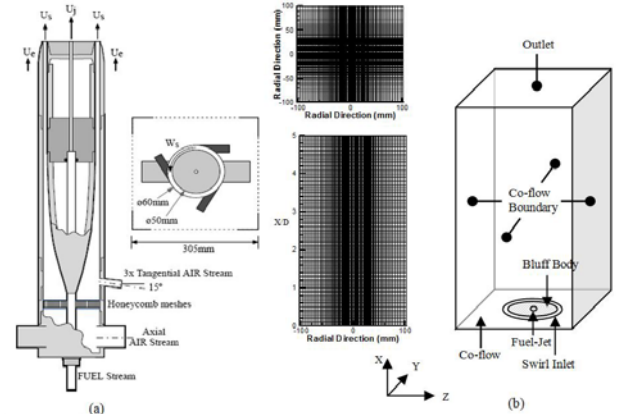


Figure 1. Experimental configuration and computational geometry.

The computational geometry and grid details used in LES calculations are depicted in the Figure 1(b). The computational domain has dimensions of 200 x 200 x 250 (all dimensions are in mm). The axial distance of approximately 70 jet diameters and the burner width of approximately 55 jet diameters are used in order to account the independency of flow entrainment from the surroundings. The inlet jet velocity is specified with a 1/7th power law profile.

A Cartesian staggered non-uniform grid distribution of 100 x 100 x 100 in the X, Y and Z directions is used to discretise the domain.

Case	$U_j$	$U_s$	$W_s$	$Re_j$	$S$
SMH1	140.8	42.8	13.8	19300	0.32

Table 1: SMH1 properties

### Sydney Experimental Explosion Chamber

The experimental test cases used to validate the LES predictions of explosion deflagrating flames are those, reported by The University of Sydney combustion group (Kent et al, 2005). A schematic diagram of the laboratory scale explosion rig, with baffle plates and a solid square obstacle is illustrated in Fig. 2. The chamber is made of 50 mm square cross section with a length of 250 mm and having a total volume of 0.625 litres. This chamber has the capability to hold a deflagrating flame in a strong turbulent environment, generated due to the presence of solid obstacles at different downstream locations from the bottom ignition end. It is designed in such a way that locations of the baffle plates could be varied to construct several configurations of baffle arrangements with the standing square solid obstacle in the path of the deflagrating flame. These baffle stations are named as S1, S2 and S3 and located at 20, 50 and 80 mm respectively from the ignition point as shown in Fig. 2.

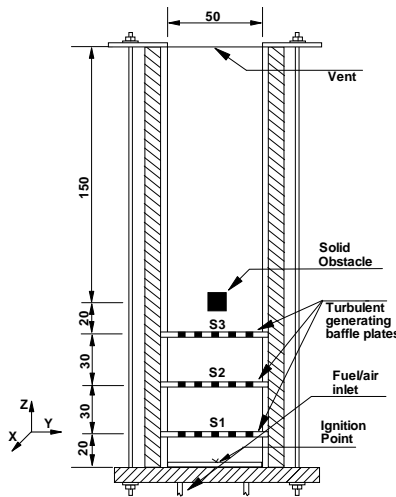


Figure 2

Each baffle plate is of 50 x 50 mm, aluminium frame, constructed from 3 mm thick sheet, consisting of five 4 mm wide bars each with a 5 mm wide space spreading them through out the

chamber. A solid square obstacle of 12 mm cross-section is centrally located at 96 mm from the bottom ignition end of the chamber. Depending on the location, the number of baffles and their positions, configurations shown in Fig. 3 have been used in the experiments. To aid the analysis and the discussion of the results various families of these configurations have been identified. Table 2 below shows a number of families that could be categorised. Simulation results for family 1 and 3 are presented and discussed briefly in this paper. Configuration 0 is the basic or trivial configuration without any obstacle plates. This configuration is also considered in the simulations.

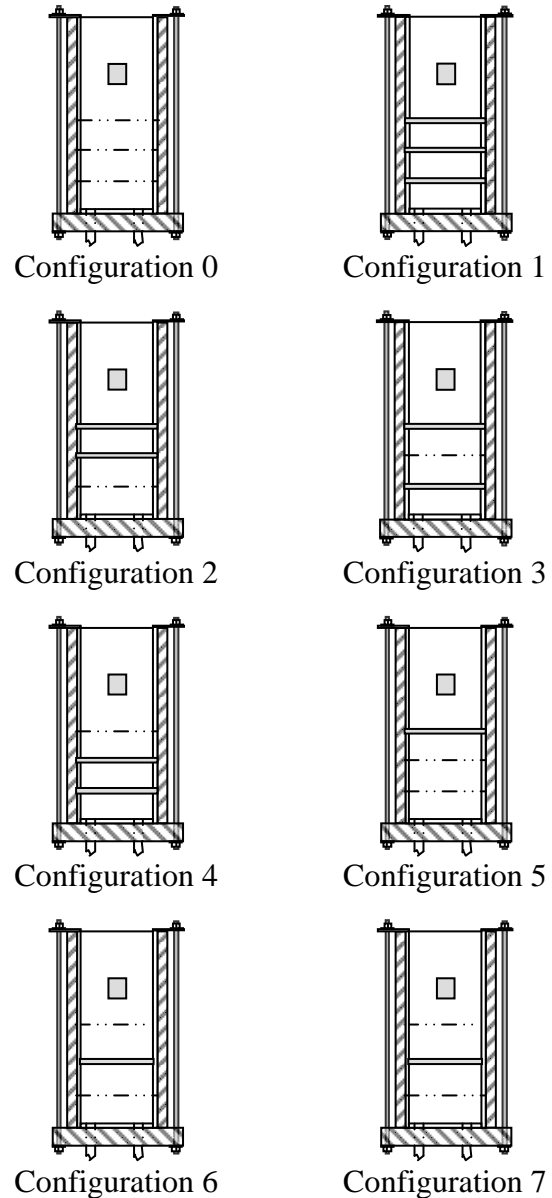


Figure 3 All configurations

Family name	Configurations and order
Family 1	5 – 2 – 1
Family 2	1 – 7 – 4
Family 3	2 – 3 – 4
Family 4	6 – 7 – 0

Table 2 – Families of configurations

## RESULTS AND DISCUSSION

### LES Modelling of Non-premixed Swirl Combustion : SMH1 Flame

This section presents sample of results from various numerical simulations performed for the SMH1 swirl flame. In order to identify the resulting differences between inclusion and non-inclusion of radiation, simulations were performed with and without radiation. In the discrete transfer method 16x16 number of rays were used for angular discretisation. Coupling of radiation with the laminar flamelet model was achieved by incorporating the enthalpy defect technique previously used in other RANS based calculations (Hossain et al, 2001, Ravikanti-Veera et al, 2008,).

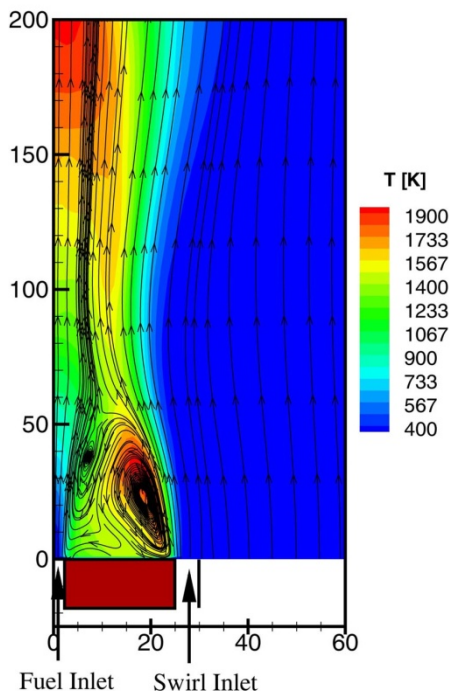


Fig. 4 Stream traces of axial velocity plotted with temperature contours at the central plane

LES simulation including radiation is identified as NAFM (non adiabatic flamelet model) and the calculation without radiation is identified as AFM (adiabatic flamelet model). It should be noted that both models are based on the steady laminar flamelet model for non-premixed combustion.

Swirl flames exhibits complex flow features in terms of various recirculation zones and these features are important in flame stabilization. Fig. 4 shows the LES predicted mean flow pattern with stream traces of axial velocity plotted on temperature contours. Numerical results correctly predict two bluff body recirculation zones. These two counter rotating vortex zones lead to a high temperature region above the bluff body. Detailed results are presented for velocity flow field, temperature, mixture fraction and species mass fractions and compared with respective experimental data. Comparison of predicted axial and swirl velocity components compared with the experiments at various axial locations are shown in Fig. 5 and 6. It can be seen that LES results agree well with the experimental data indicating that overall flow features in this complex swirl flow situation have been predicted well by the LES based combustion model. LES resolves the axial velocity component very well at all locations except at one downstream location  $z/D=2.5$ . This location corresponds to the axial vortex breakdown region of this swirl flame and therefore flow is highly unstable. Because of this highly unstable nature current LES technique does not completely capture the exact flow and flame properties and this could well be a result of the deficiencies of the steady laminar flamelet concept which does not include transient, extinction and re-ignition effects. In Fig 6 the correct development of the swirl velocity pattern at radial distance of  $r/R = \{1.0-1.2\}$  at the initial three axial locations are captured well with both combustion models (NAFM and AFM). However, the discrepancies in the predictions can be found at further downstream locations. Again these discrepancies correspond to the highly unstable and transient region of the flame. Comparison of the results of NAFM and AFM shows that the effect of radiation on the flow field is minor. There are slight differences between inclusion and non-inclusion of radiation.

Predictions with radiation show slightly closer agreement at most locations.

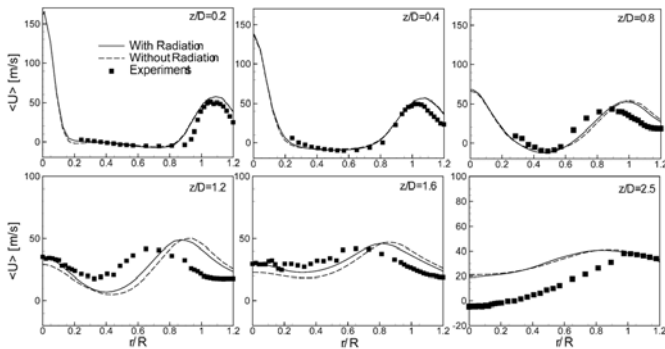


Fig. 5 Radial plot for axial velocity at different axial locations

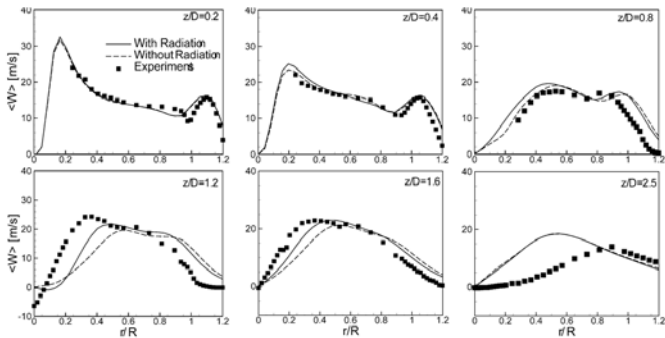


Fig. 6 Radial plot for swirl velocity at different axial locations

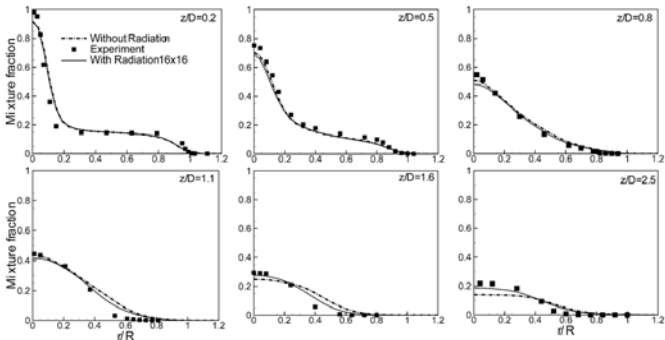


Fig. 7 Radial plot for mixture fraction at different axial locations

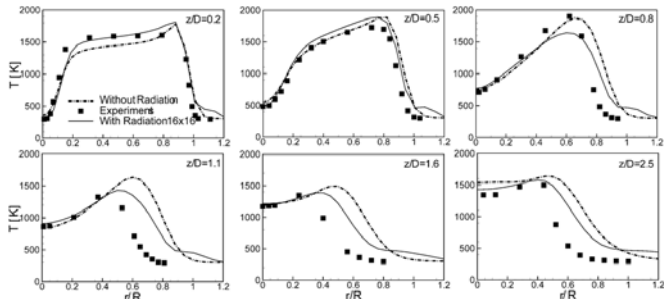


Fig. 8 Radial plot for temperature at different axial locations

Performance of NAFM and AFM model are further assessed through the comparison with other experimental data. Fig. 7 shows the predictions of mean mixture fraction from both models compared with measurements. The figure shows very close agreement with the experiments and both models show very similar results. Results including radiation show slightly better agreement at downstream locations.

Predicted radial profiles of mean temperature at various axial locations are compared in Fig. 8. Here inclusion of radiation shows a clear difference. It can be seen that NAFM which include radiation effects predict closer agreement than the AFM (without radiation). There is noticeable difference between the two results. Both models tend to over predict at downstream locations but NAFM with the radiation heat losses predict slightly closer to the experiments. It could be said that inclusion of radiation in LES calculation improves the overall quality of the results. At downstream axial locations radiation losses result in a drop in temperatures when compared with the adiabatic model hence the predictions are much closer to the measurements.

The contour plot of temperature for both models is shown in Fig. 9. These contour plots show that there are three recirculation zones as observed in the experiments, two above the bluff body region and one central vortex breakdown region along the axis downstream of the flame. Both models predict these flow features very well. However, it is observed that there is a considerable shift in the temperature contours towards further down-stream in the case with radiation. As seen in radial plots at any axial location NAFM gives lower temperatures compared to the predictions of AFM adiabatic model. Therefore inclusion of radiation effects is clearly seen from the differences in temperature pattern. The radiation losses due to major emitting species such as  $\text{CO}_2$  and  $\text{H}_2\text{O}$  are the main source of this temperature drop. The most important observation is that the flame diffuses more in the radial direction with the inclusion of radiation calculations. This is basically due to radiation emission from high temperature product species slightly lower the local temperature and the emitted energy is absorbed in the other regions.

Without the inclusion of radiation this effect is not accounted for.

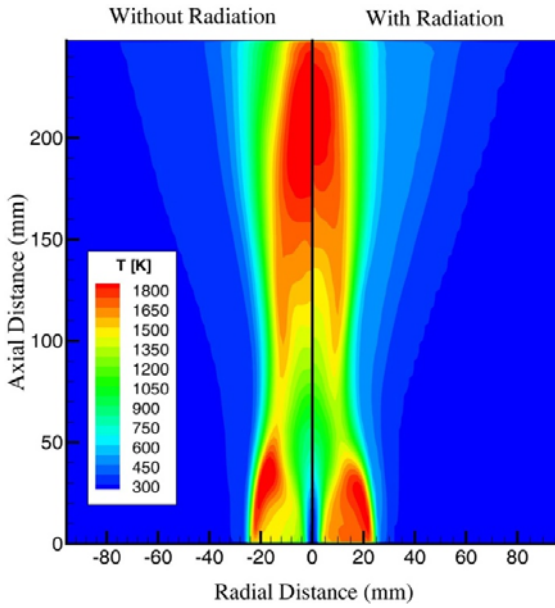


Fig. 9 Mean temperature plot at the centre plane (a) Without radiation (left) (b) With radiation (right)

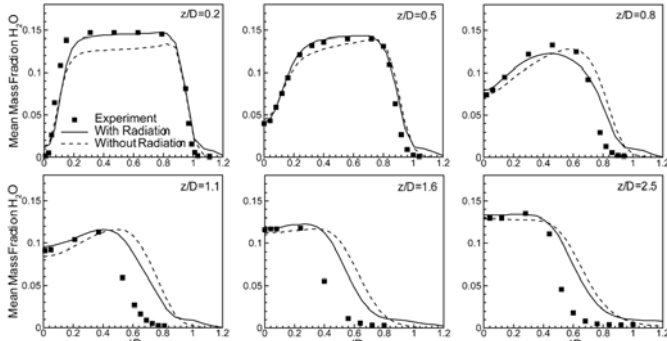


Fig. 10 Radial plot for mean mass fraction of H<sub>2</sub>O at different axial locations

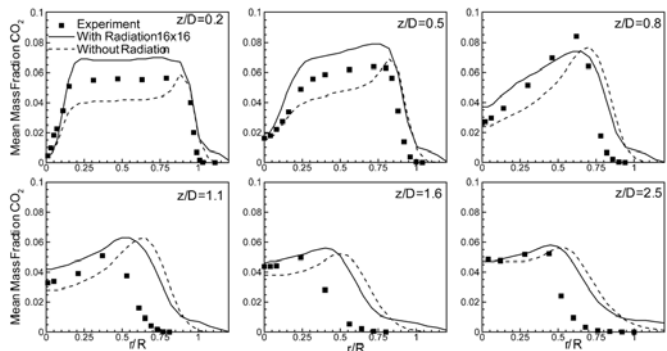


Fig. 11 Radial plot for mean mass fraction of CO<sub>2</sub> at different axial locations

Figures 10 and 11 show the predictions of mass fraction of H<sub>2</sub>O and CO<sub>2</sub> respectively compared

with experiments. Fig. 10 shows H<sub>2</sub>O radial mass fractions. It can be seen that predictions with the NAFM model which include radiation are better than the AFM results. Similar observation can be made in CO<sub>2</sub> predictions (Fig. 11). At first three locations under prediction of CO<sub>2</sub> profiles seen with the AFM are much improved with NAFM calculations. Although they are slightly over-predicted at downstream locations, NAFM shows better agreement with the experimental data.

In general LES results show quite good agreement with experimental results and show the ability of the technique in predicting flame properties of this complex swirl flow situation. As mentioned there are still some deficiencies in the model. These could be due to various reasons. Improvements to sub-grid scale combustion modelling and more fine grid resolutions for LES can possibly improve these. It is fair to note that the laminar flamelet model may not be the ideal model to use in highly turbulent dynamic situations. Transient flamelet models or models that incorporate extinction and re-ignition effects incorporated into LES could provide better results than the present calculations. However, the present calculations demonstrate that LES as a combustion modelling technique is quite successful and very useful for complex flow configurations.

### LES Modelling of Premixed Propagating Flame over Obstacles

Results from the LES simulations of stagnant, stoichiometric propane/air deflagrating flames over solid obstacles are presented and discussed in this section. A novel DFSD model (Knikker et al, 2004, Ibrahim et al, 2009) to account for the SGS chemical reaction rate is used to model premixed combustion in the vented chamber geometries shown in Fig. 3. Four families as identified in Table 2 were analysed for flame dynamics, structure and other combustion characteristics. In each case baffle plates and the solid square obstacle used inside the chamber are aimed to generate turbulence by disrupting the flame propagation with different blockage ratios. A sample of results from six flow configurations are presented and discussed here to highlight the success of the LES based modelling technique. Primary objective of the present work is

the application of DFSD model in predicting the turbulent premixed flame dynamics in a wide range of flow configurations. Influence of the position of baffle plates with respect to the origin of ignition, in generating overpressure due to the interactions with deflagrating flames, is also examined.

**Flame Characteristics: Configuration 0**

Configuration 0 has no baffles except a solid square obstacle in the centre of the chamber. Since, baffles are not present in this chamber, the flame takes longer to encounter the central solid obstacle and to reach blow-down stage, than in any other configuration to be discussed later. Comparison of LES predictions with the time series of overpressure and flame position are shown against experimental measurements in Figure 12. It can be seen that LES predictions show excellent agreement with measurements from ignition to blow-down, including the time of pressure rise at about 11.5 ms, slope of pressure rise, peak pressure and its incidence time at 13.5 ms. Here LES predicted peak overpressure is 36.6 mbar at 13.5 ms and the experimentally measured value is 34 mbar at 13.5 ms, which is slightly over-predicted by 7.6%. It is also evident from Figure 12 that the pressure reflections, once the main flame has left the chamber are also in good agreement with experiments. Similarly, the flame position shown in Figure 12 confirms this observation with an exact match of, up to peak overpressure and thereafter with a slight deviation.

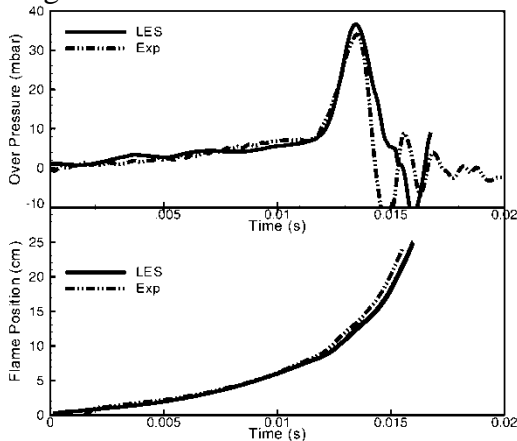


Figure 12. Time histories of overpressure and flame position for configuration 0.

Figure 13 shows sequence of flame front images from LES (reaction rate contours) and experiments (false coloured images extracted from high speed video). It is evident from these images, that the LES simulations are capable of reproducing turbulent flame structure very accurately at various stages. For instance at 12.5 ms, the flame shape (finger shape) and its approach towards square obstacle can be immediately noticed. Similarly, at 13.5 ms (peak overpressure incidence) LES capture the same shape of the corresponding experimental image i.e. flame engulfs upstream of square obstacle by trapping certain amount of unburnt mixture, which can be seen to burnt before 14.5 ms. Then the unburnt mixture trapped in recirculation zone burn after main flame has left the chamber, resulting in pressure reflections at a later stage.

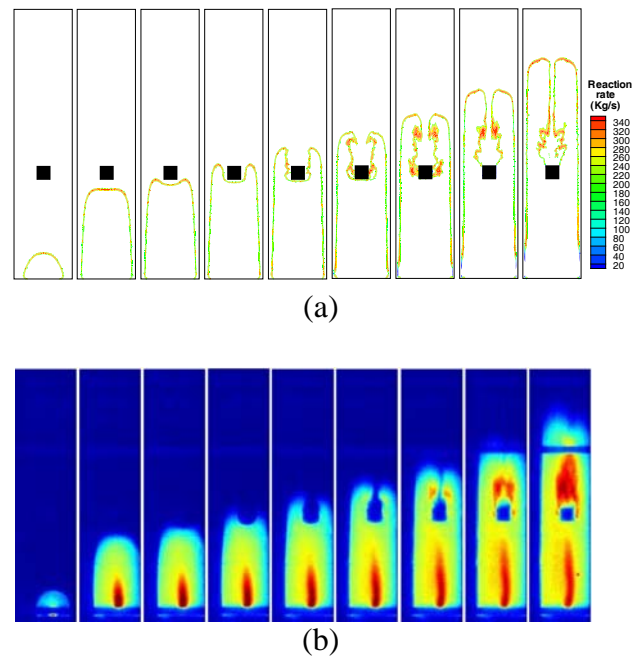


Figure 13. Series of flame images at 6.0, 12.0, 12.5, 13.0, 13.5, 14.0, 14.5, 15.0, 15.5 ms respectively after ignition (a) LES (b) Experimental video images (false coloured).

**Flame Characteristics: Family 1**

Family 1 consists of configurations 5-2-1 with progressively increasing number of baffles from one to three and positioned farthest from ignition bottom as shown in Fig. 3.

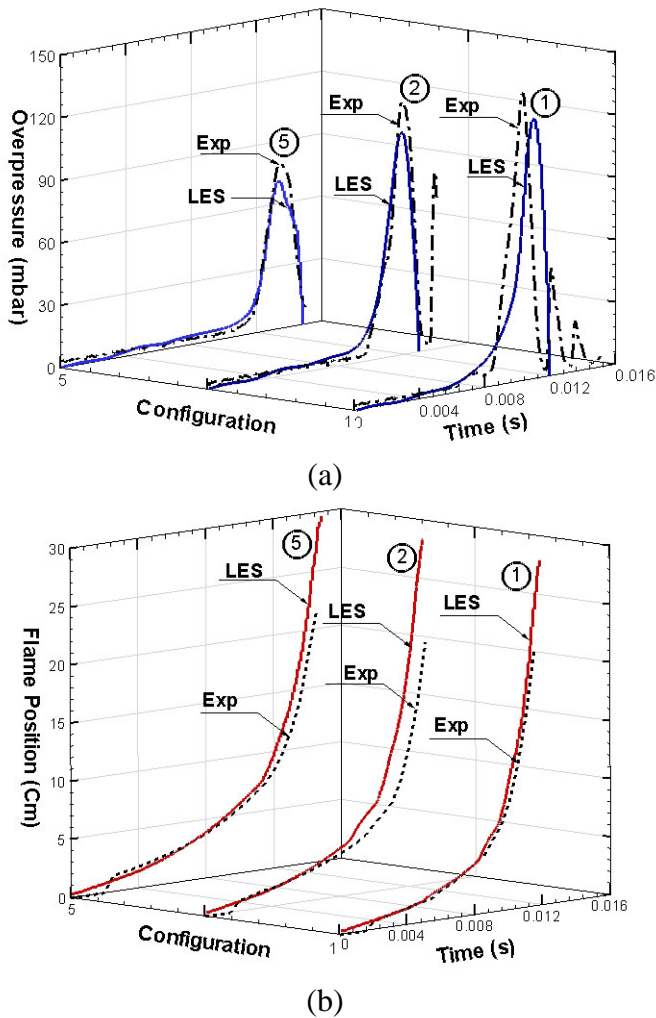


Figure 14. Comparison of predicted and measured time traces of Family 1 (a) overpressure (b) flame position.

For this family of configurations LES results of time histories of overpressure and flame position compared with experimental data are shown in Fig. 14 (a) & (b) respectively. It is evident from Fig. 14(a) that the predicted overpressure trend is in excellent agreement with data with slight under-prediction of peak pressure in all three configurations. Figure 14(a) also highlights the impact of the number of baffles and their position with respect to distance from the ignition bottom. The time elapsed in reaching the first baffle from the ignition bottom and increase in the steepness of pressure gradient due to the generated turbulence can be noticed. For example Configuration 1 which has three obstacles results in the highest peak pressure. LES predicted flame position shown in

Fig. 14(b) also compare well with data except for configuration 2 where there is a slight discrepancy. It should be noted that in the case of experiments, the flame position is extracted from high speed video images by locating the farthest location of the flame front from ignition bottom end. From LES calculations, the flame position is obtained by locating the farthest location of the leading edge of the flame front from the bottom end (defined here as the most down stream location of the flame, where  $c = 0.5$  from the ignition point).

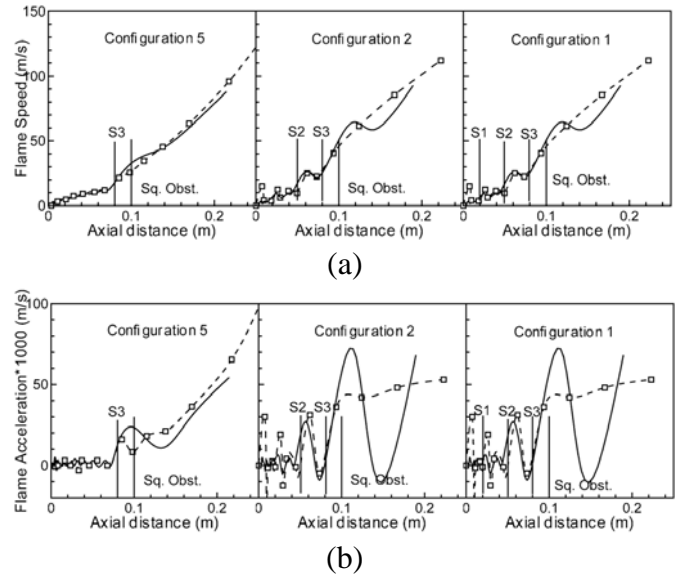


Figure 15. Comparisons of predicted (Solid line) and measured (Dashed lines with square symbols) (a) flame speed (b) flame acceleration The location of baffle stations (S1, S2 and S3) and the square solid obstacle are shown.

Figures 15 (a) and (b) show comparison of flame speed and acceleration respectively from LES and experiments. It can be seen that the flame speed and acceleration from LES are in very good agreement with experimental measurements, except when the flame is located downstream of the square obstacle in blow-down region. One main reason for this is due to the limitation in the resolution of experimental measurements. Within blow-down region, the flow conditions are highly turbulent and flame propagates faster with approximately about 80-100 m/s in this family.

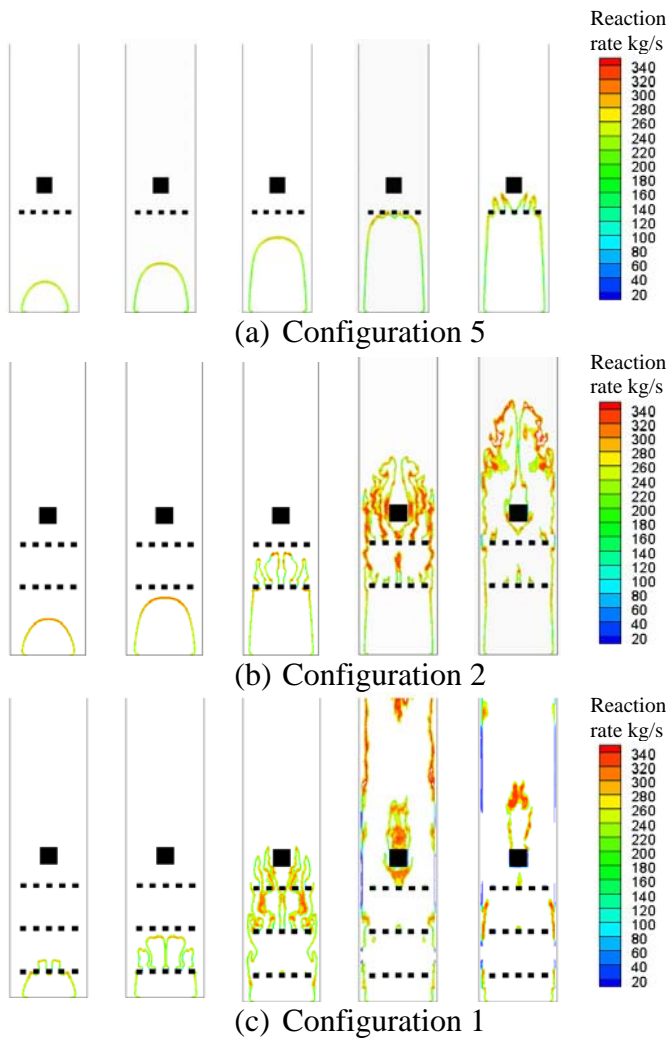


Figure 16. Predicted flame structure in each configuration at times 6, 8, 10, 11.5 and 12.0 ms after ignition.

Figure 16 (a-c) presents cut-views of LES predicted reaction rate contours, showing flame structure at 6.0, 8.0, 10.0, 11.5 and 12.0 ms after ignitions for this family. This facilitates qualitative and quantitative comparison of flame position and its structure at any given time within this family. For instance at 8.0 ms from ignition Figure 16 (c) illustrates the finger shaped flame structure, which is generally expected in chambers having  $l/d$  ratio greater than 3. Fig. 16(b) at 11.5 and 12.0 ms shows a clear picture of entrapment of unburnt fuel/air mixture around solid square obstacle within the recirculation zone. Similar pockets or traps in the case of configuration 1 in Fig. 16(c) at times 10.0 and 11.5 ms are clearly noticeable. Similarly, Fig.

16(c) at 11.5 and 12.0 ms shows the consumption of trapped mixture, once the main flame had left the chamber. Comparison of plots gives an insight into how flame acceleration occurs and it could be used to explain how overpressure is generated in a given configuration.

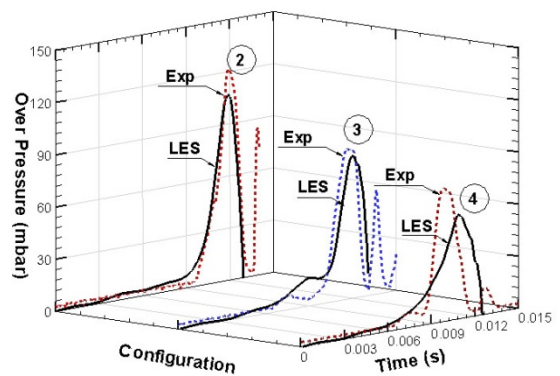
### Flame characteristics: Family 3

Family 3 has three configurations i.e. 2-3-4 with two baffle plates at different stations and a solid square obstacle at the fixed position. Figure 17 (a) and (b) shows characteristic comparison of overpressure and flame position respectively for these three configurations, and experimental measurements and LES simulations are compared. It is evident from Fig. 17 (a) that the rate of pressure rise and its trend including first hump are predicted well except for configuration 4, where the computed rate of increase of pressure is slower than measurements indicating a faster decay of turbulence between the second baffle plate and the square obstacle. Figure 17 (b) shows the flame position predictions. Very good agreement can be seen for all configurations. In configuration 3 predictions overlaps with the experimental data and a slightly faster propagation rate across the chamber is seen in configurations 2 and 4. It should be noted here that this phenomenon is only observed in the last few milliseconds of propagation where the flame is experiencing the highest levels of turbulence.

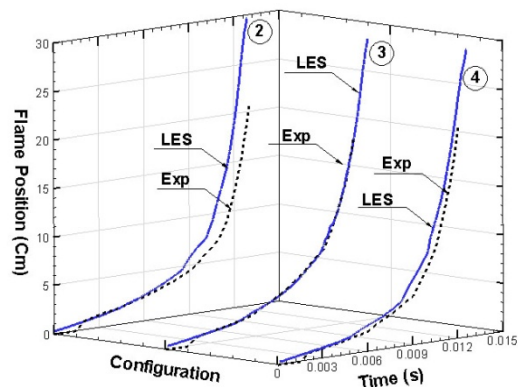
Figure 18 (a) and (b) show comparison between experimental measurements and numerical predictions of flame speed and acceleration. Figure 18 also shows the position of baffle plates and the solid square obstacle to identify the influence of the obstacles. The predictions capture the correct trend and behaviour seen in the experimental data. Highest flame speed and acceleration are recorded at the square obstacle in configuration 2 than other two configurations. It is also interesting to note that, in configuration 4, the slowdown in flame speed and acceleration between the second baffle plate and the square obstacle is due to relatively longer distance compared to other configurations in this family (see Fig. 3).

Figure 19 (a-c) shows the reaction rate contours at various instances in this group. At 6ms, the flame is seen to be jetting out of the first baffle in configurations 3 and 4. In contrast at 6ms, the flame in configuration 2 is seen to be relatively smooth. Similarly, the flame in configuration 2 and 3 can be seen to be interacting with baffle plate at S3 having a different flame structure at 10ms. Figures 19 illustrates quicker flame exit in configuration 4 than in configuration 2. Though, the flame in configuration 2 propagates at lower speed at the beginning, it becomes highly turbulent due to jetting and contortion through repeated baffles. In configuration 3, the flame is found to be distorted as it reaches the first baffle. However, re-laminarisation of the flame between S1 and S3 results in approaching the square obstacle at a later stage compared to configuration 4. These flame interactions results in the changes in flame speed and contribute to the pressure rise. In general this kind of LES predictions gives a good insight into flame obstacle interactions.

From the results presented above it can be concluded the novel DFSD model is successful in predicting the flame behaviour, structure; position and other characteristics and they are in agreement with experimental measurements. Generally predicted overpressure-time trend for all configurations are in good agreement with data although slight under-prediction can be seen for some configurations. In all configurations LES results have correctly reproduced experimentally observed flame position, flames speeds, and flame acceleration trends. LES results are also very useful in interpreting how obstacles interact with the propagating flame. This investigation demonstrates the effects of placing multiple obstacles at various locations in the path of the turbulent propagating premixed flame. As expected, calculations show that the increase in blockage ratio increases the overpressure, however, with same blockage ratio, the position of solid obstruction with respect to each other and ignition end has a significant impact on the magnitude of the overpressure and spatial flame structure.



(a)



(b)

Figure 17. Family 3: Comparison of predicted and measured (a) overpressure (b) flame position.

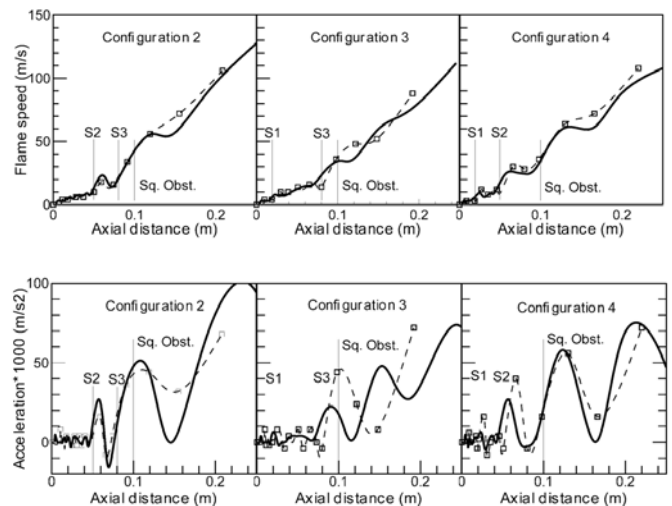


Figure 18. Comparisons of predicted (Solid line) and measured (Dashed lines with square symbols) (a) flame speed (b) flame acceleration The location of baffle stations (S1, S2 and S3) and the square solid obstacle are shown.

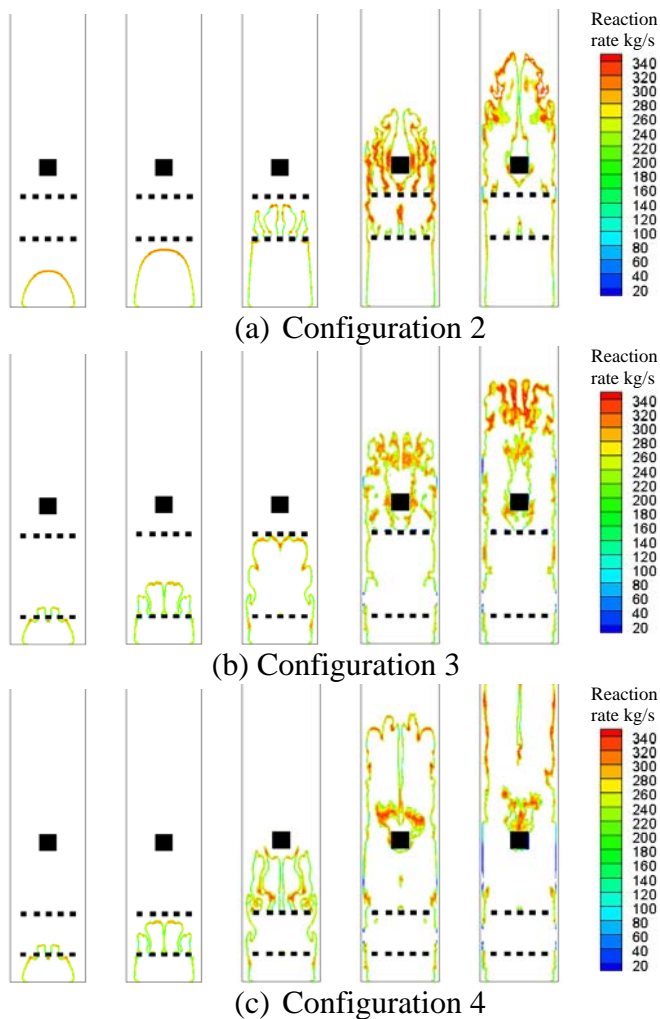


Figure 19. Predicted flame structure in each configuration at times 6, 8, 10, 11.5 and 12.0 ms after ignition.

## SUMMARY

In this paper we have shown how LES could be applied with appropriate models to compute premixed and non-premixed combustion situations. A complex swirl flame was considered as an example for non-premixed modelling. It was demonstrated that LES based combustion modelling showed very encouraging results in terms of resolving complex features of the swirl flow considered and predicted results showed good agreement with data. A propagating flame over obstacles was considered for the demonstration of premixed combustion modelling. In this work a novel DSFD model was used in the LES modelling. Comparison of results showed excellent agreement

with data demonstrating the ability of LES. Overall it could be concluded that LES is a very useful tool for accurate modelling of premixed and non-premixed reacting flows and expected to grow in the future as it could produce an accurate account of the flow and combustion characteristics.

## REFERENCES

- Branley, N and Jones, W.P., 2001, Large eddy simulation of a turbulent non-premixed flame, *Comb. Flame*, 127, 1914-1934.
- Bowman, C.T, Hanson, R. K, Davidson, D. F, Gardiner, W. C, Lissianki, V, Smith, G. P, Golden, D. M, Frenklach, M, Goldenberg, M., 2006, GRI 2.11, [http://www.me.berkeley.edu/gri\\_mech](http://www.me.berkeley.edu/gri_mech)
- Charlette, F., Meneveau, C., and Veynante, D., 2002, A power-law flame wrinkling model for LES of premixed turbulent combustion Part II: Dynamic formulation, *Comb. and Flame*, 131, 181-197.
- Di Mare, Jones. W. and Menzies. K., 2004, Large eddy simulation of a model gas turbine combustor, *Combust. Flame*, 137(3), 278-294.
- Escudier, M., 1988, Vortex breakdown: observations and explanations, *Prog. Aero. Sci.*, 25, 189-229.
- Fureby, C., Pitsch, H., Lipatnikov and Hawkes, E., 2005, A fractal flame-wrinkling large eddy simulation model for premixed turbulent combustion, *Proc. of the Combustion Institute*, 30(1), 593-601.
- Gubba, S.R., Ibrahim, S.S., Malalasekera, W. and Masri, A.R., 2008, LES modelling of premixed deflagrating flames in vented explosion chamber with a series of solid obstructions, *Comb. Sci. Tech.*, 10 (180), 1936-1955.
- Gupta, A.K., Lilly, D.G and Syred, N., 1984, *Swirl Flows*, Abacus Press, Kent, England.
- Henson, J.C., 1998, Numerical Simulation of Spark Ignition Engines with Special Emphasis on Radiative Heat Transfer, Ph.D. thesis, Loughborough University, UK.
- Henson, J.C. and Malalasekera, W., 1997, Comparison of discrete transfer and Monte-Carlo methods for radiative heat transfer in three-dimensional non-homogeneous scattering media,

- Num. Heat Transfer Part A: Applications, 32(1), 19-36.
- Hossain, M., Jones, J.C. and Malalasekera, W., 2001, Modelling of a Bluff-Body Nonpremixed Flame Using A Coupled Radiation/Flamelet Combustion Model, *Flow Turb. and Combustion*, 67, 217-234.
- Ibrahim, S.S, Gubba, S.R., Masri, A.R. and Malalasekera, W., 2009, Calculations of Explosion Deflagrating Flames using a Dynamic Flame surface density Model, *a Journal of Loss Prevention in the Process Industries*, 22(3), 258-264.
- Kent, J. E., Masri, A. R., and Starner, S. H., 2005, A new chamber to study premixed flame propagation past repeated obstacles, Paper presented at the 5th Asia-Pacific Conference on Combustion, The University of Adelaide, Adelaide, Australia (2005).
- Kim, W, Menon. S. and Mongia, H.,1999, Large eddy simulation of a gas turbine combustor flow, *Combust. Sci. Tech.*, 143, 25-63.
- Knikker, R., Veynante, D., and Meneveau, C., 2002, *Proc. Combust. Inst.*, 29, 2105-2111.
- Knikker, R., Veynante, D. and Meneveau, C., 2004, A dynamic flame surface density model for large eddy simulation of turbulent premixed combustion, *Physics of Fluids*, 16(11), L91-L94.
- Lockwood, F. C. and Shah, N. G., 1981, A New radiation Solution method for Incorporation into General Combustion Prediction Procedures, 18th Symp. (Int.) on Comb., The Combustion Institute, 1405-1414.
- Lucca-Negro, O. and O'Doherty, T.O., 2001, Vortex breakdown: a review, *Prog. Ener. Comb. Sci.*, 27, 431-481.
- Malalasekera, W. and James, E.H., 1996, Radiative Heat Transfer Calculations in Three-Dimensional Complex Geometries, *J. of Heat Transfer*, 118, 225-228.
- Mahesh, K, Constantinescu, G, Apte, S, Iaccarino, G, Ham, F. and Moin, P., 2000, Large eddy simulation of turbulent flow in complex geometries, *ASME J. App. Mech.*, 73, 374-381.
- Masri, A.R., Ibrahim, S.S., and Cadwallader, B.J., 2006, *Experimental Thermal and Fluid Science*, 30, 687-702.
- Moin, P., Squires, K., Cabot, W., and Lee, S., 1991, A dynamic subgrid-scale model for compressible turbulence and scalar transport. *Physics of Fluids*, A3, 2746-2757.
- Patel, S.N.D.H, Jarvis, S, Ibrahim S.S. and Hargrave, G.K., 2002, An experimental and numerical investigation of premixed flame deflagration in a semiconfined explosion chamber, 29(2), 1849-1854.
- Pitsch, H., 1998, A C++ computer program for 0-D and 1-D laminar flame calculations, RWTH, Aachen.
- Pitsch, H., 2005, A consistent level set formulation for large-eddy simulation of premixed turbulent combustion, *Combustion and Flame*, 143(4), 587-598.
- Pitsch, H., 2006, Large-eddy simulation of turbulent combustion, *Annual Review of Fluid Mechanics*, 38, 453-482.
- Pitsch, H., and De Lageneste, D., 2002, Large Eddy simulation of premixed turbulent Combustion using a level-set approach, *Proc. Combust. Inst.*, 29, 2001-2008.
- Piomelli, U. and Liu, J., 1995, Large eddy simulation of channel flows using a localized dynamic model, *Phy. Fluids*, Vol. 7, pp. 839-848.
- Ravikanti-Veera, M.M.R, Malalasekera, W. and Hossain, M, 2008, Flamelet Based NO<sub>x</sub>-Radiation Integrated Modelling of Turbulent Non-premixed Flame using Reynolds-stress Closure, *Flow, Turbulence and Combustion*, 81 (1/2), 609-612.
- Sankaran, V, Menon, S., 2002, LES of spray combustion in swirling flows, *J. Turbulence*, 3, 11-23.
- Shah, N. G., 1979, The computation of radiation heat transfer, PhD Thesis, Imperial College, London.
- Sloan, D.G., Smith, P.J. and Smoot, L.D., 1986, Modelling of Swirl in Turbulent Flow Systems, *Prog. Energy Combust Sci.*, 12, 163-250.
- Smagorinsky, J., 1963, General circulation experiments with the primitive equations, *Monthly Weather Review*, 91(3), 99-164.
- Syred, N and Beer, J.M., 1974, Combustion in Swirling Flows: A Review, *Combust. Flame*, 23, 143-201.

- Truelove, J. S., 1976, A Mixed Grey Gas Model for Flame Radiation, AERE Harwell, Oxfordshire, UK.
- Veynante, D., and Poinso, T., 1997, Large eddy simulations of the combustion instabilities in turbulent premixed burners. Annual research briefs, Center for turbulence research. 253-275.
- Wall, C.T and Moin, P., 2005, Numerical methods for Large eddy simulation of acoustic combustion instabilities, Tech. Rep. TF.91. Stanford University, CA.
- Weber, R, Visser, B.M, Boysan, F., 1990, Assessment of turbulent modelling for engineering prediction of swirling vortices in the near burner zone, Int. J. Heat and Fluid Flow, 11, 225-238.